

# Synergy and competition in nano- and micro-design of structural ceramics

A. Bellosi\*, D. Sciti, S. Guicciardi

*CNR-ISTEC, Via Granarolo 64, 48018, Faenza, Italy*

## Abstract

Nanosized structural ceramics SiC and  $\text{Al}_2\text{O}_3$ -SiC composites were produced and studied in order to define relationships among micro-structures (in the micro- and nano-size range) and mechanical properties. In both the systems, no evident improvement in strength and toughness was associated to nano-structures in comparison to micro-structures. However, nano-indentation tests on liquid-phase sintered SiC reveal peculiar and distinctive properties of nanostructured ceramics that imply unexpected repercussions for application performances involving the contact between two materials.  $\text{Al}_2\text{O}_3$ -SiC nano-composites have lower friction coefficient and higher wear resistance than the pure alumina. The advantages of nano-ceramics are attributed either to the higher grain boundary strength, as in the case of the nano-composites or to surface-dependent deformation mechanisms, like grain boundary sliding, in nanosized monolithic ceramics.

© 2003 Elsevier Ltd. All rights reserved.

**Keywords:**  $\text{Al}_2\text{O}_3$ -SiC; Mechanical properties; Microstructure-final; Nanocomposites; SiC

## 1. Introduction

During the last few years, the design of engineering ceramic materials, as many other high-tech materials, has been focused on the transition from micro-structure to nano-structure. The manufacturing of nano-structured ceramics implies a complete revision of the processing procedures concerning either powder treatments or sintering in order to maintain the grain size characteristic of the initial powder. The main technological problems are related to the high specific surface area of nanosized powders that favours surface contamination and oxidation, low packing density, easy particle agglomeration. This last feature causes consequent different grain growth during sintering and therefore the powder treatment is one of the key stages to be controlled during manufacturing. Conventional sintering and pressure-assisted sintering are often not acceptable due to intensive recrystallization process, unless a careful control of the processing parameters is attempted to increase the ratio densification/grain growth. In fact, the potential benefits in term of properties and performance can be exploited provided that microstructure optimization is carefully pursued. Innovative properties of nanostructured ceramics regard: high temperature

super-plasticity; peculiar thermal and mechanical properties, improved wear resistance, tailored functional properties, etc. Some of the properties depend on bulk characteristics, other properties depend mainly on surface properties and/or on the relationships among composition and morphology of the phases constituting the materials. Actually, for structural applications, mechanical properties generally are related to several microstructural features, and so far many contradictory results are reported in literature concerning the relationships between grain size and strength, toughness, hardness, etc.

The present work highlights some relationships between microstructure and properties of two ceramic systems for structural applications: nanostructured monolithic silicon carbide<sup>1–3</sup> and nanocomposites alumina/silicon carbide.<sup>4–8</sup> In the specific instance, several mechanical properties were measured and compared on materials with different microstructures. Besides, nano-structured silicon carbide was tested by nano-indentation technique and, for  $\text{Al}_2\text{O}_3$ -SiC nanocomposites, the wear behaviour was investigated.

## 2. Nano-size silicon carbide

### 2.1. Microstructure and mechanical properties

Fully dense SiC ceramics were produced through liquid phase sintering,<sup>3</sup> that was permitted by the

\* Corresponding author. Tel.: +39-546-699-759; fax: +39-546-46381.  
E-mail address: [bellosi@istec.cnr.it](mailto:bellosi@istec.cnr.it) (A. Bellosi).

addition of suitable sintering aids (7 wt.%  $\text{Al}_2\text{O}_3$  + 3 wt.%  $\text{Y}_2\text{O}_3$ ) using the hot pressing technique ( $T=1850$ – $1870$  °C and  $P=30$  MPa). Two different silicon carbide nano-powders (produced through plasma synthesis (PS) and laser synthesis (LS), respectively at PCT, Latvia and CEA-Saclay, France) were used and compared to a commercial powder (C). Their characteristics, Table 1, are related to the production procedures: plasma synthesis favours bimodal grain size distribution while laser synthesis allows very fine and uniform particle morphology.<sup>3</sup>

The SEM micrographs of plasma etched surfaces of the hot pressed samples (Fig. 1) evidence the different grain size depending on the raw powder characteristics: the product from commercial powder has mean grain size of 540 nm, while grain refinement up to 140 and 80 nm were obtained starting from the powders having 60 and 30 nm mean particle size, respectively.

Different grain boundary phases were observed in the hot pressed materials (Figs. 2a,b) depending on the raw powders:<sup>3</sup> amorphous phase amounts of 5, 15, 7 vol.% were estimated in materials from C, PS or LS powders, respectively. The mean composition (at.%) of the glassy phase in the dense silicon carbide from LS is: 64 O, 10

Al, 10 Y and 16 Si and in the material from PS powder: 62 O, 6 Al, 6 Y, 25 Si. In addition, about 9 vol.% of crystalline mullite was detected in the material produced from LS SiC and about 5 vol.% of YAG in the sample from C powder.

Table 2 summarizes the mechanical properties, that were discussed in details in previous works.<sup>3,9</sup> The room temperature flexural strength and the fracture toughness of the three materials are similar. As a consequence, also the defect population governing the room temperature strength is not very different. Actually, the use of the finest powder (LS) induces a slight reduction of the room temperature strength, mainly due to powder processing defects (an example is shown in Fig. 3a). The same sample, on the contrary, has the highest strength value at 1300 °C, where a key role is played by the grain boundary phases particularly by their amount and refractoriness. In fact the material from the laser synthesized powder contains crystalline grain boundary phases that are more refractory than glassy phases at high temperatures. In addition, the strength decrease at high temperature of all the samples is also affected by surface oxidation that increases the defects, as evidenced in Fig. 3b.

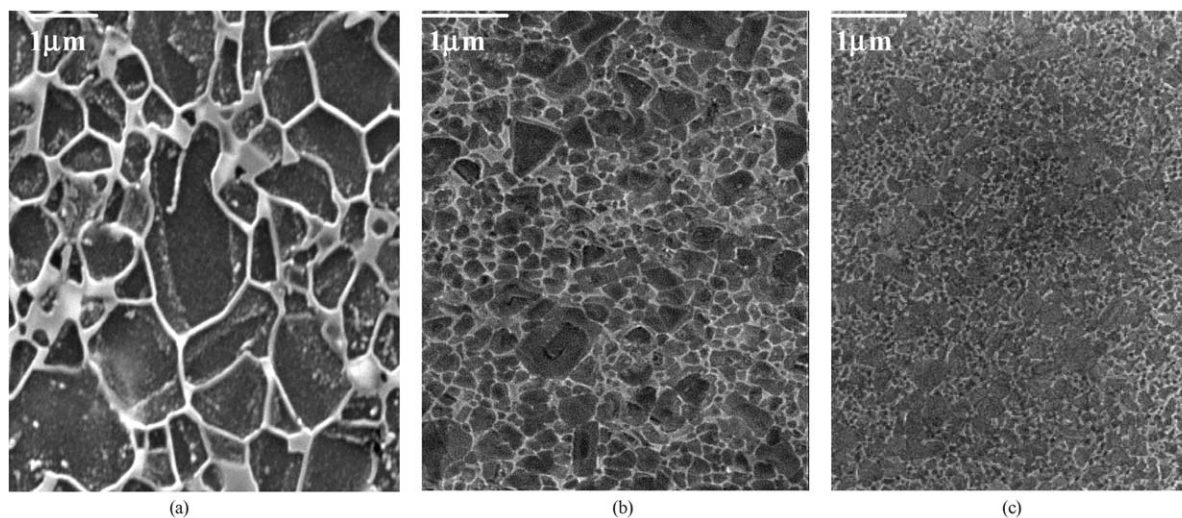
Table 1

Characteristics of the starting powders: PS plasma synthesized, LS Laser synthesized, C commercial

Powder	s.s.a. ( $\text{m}^2/\text{g}$ )	Mean grain size (nm)	$\text{SiO}_2$ content (wt%)	Crystalline phases
PS	36.2	10–20 (200–400) <sup>a</sup>	3–5	$\beta$ -SiC, $\alpha$ -SiC <sup>b</sup> , 4H and 6H, Si
LS	63	30	~7	$\beta$ -SiC, Si <sup>b</sup> , C, SiO
C	8.1	230	~2	$\beta$ -SiC (97%), $\alpha$ -SiC

<sup>a</sup> Bimodal (see text).

<sup>b</sup> Traces.



Figs. 1. SEM pictures of polished and etched surfaces of hot pressed silicon carbide, from: (a) commercial powder, (b) plasma synthesized powder, (c) laser synthesized powder.

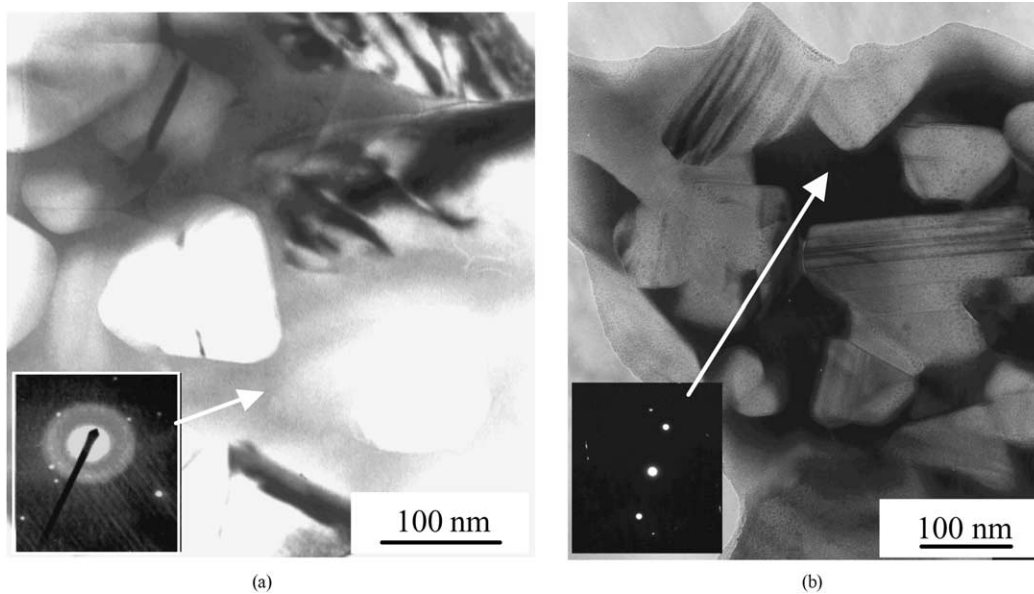


Fig. 2. (a) TEM image of the SiC hot pressed from plasma synthesised powder, revealing glassy phase in the system Si–Al–O at grain boundaries. (b) TEM image of the SiC hot pressed from laser synthesised powder, showing crystalline mullite at grain boundaries.

Table 2  
Comparison of mechanical properties of the various SiC materials

Property	Material		
	From PS powder	From LS powder	From C powders
HV (GPa)	21.9±0.3	21.9±0.5	22.0±0.8
E (GPa)	334	376	386
$K_{Ic}$ (MPa m <sup>1/2</sup> )	3.0±0.2	2.6±0.2	3.0±0.2
$\sigma$ RT (MPa)	684±90	660±65	746±56
$\sigma$ 1000 °C (MPa)	589±85	581±107	509±34
$\sigma$ 1300 °C (MPa)	158±34	243±27	148±12

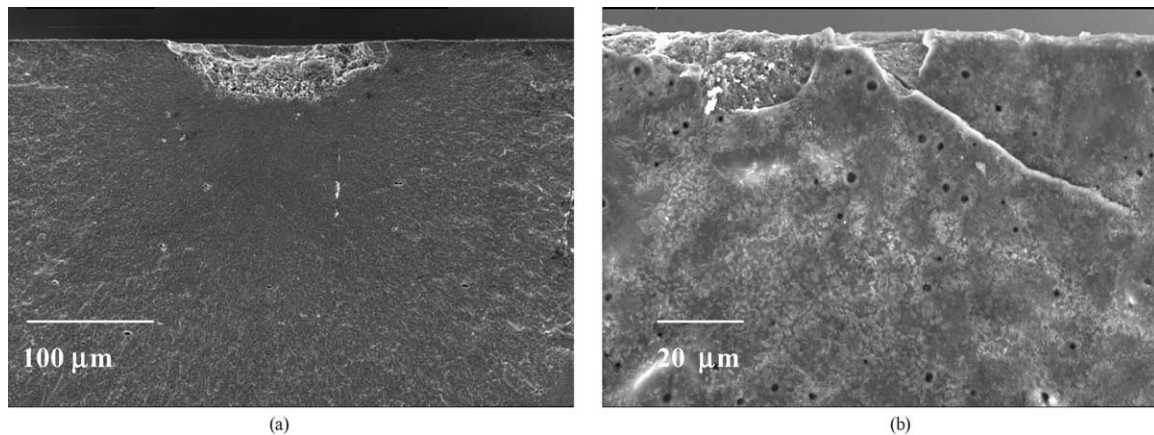


Fig. 3. (a) Critical defect at room temperature, due to scarce homogeneity of the powder mixture. (b) Critical defect at high temperature, effect of the surface oxidation.

## 2.2. The nanoindentation technique: a powerful tool to reveal distinctive and peculiar behaviours in nano-size ceramics

Nanoindentation is one of the few techniques which allow to mechanically test nano-sized materials on dimensions comparable to their microstructural scale.<sup>10–15</sup> The analysis of the nanostructured silicon carbide by nanoindentation highlighted, in comparison to sub-micro-size SiC, that:

- nanoceramics do not appear to exhibit indentation size effect (ISE); a load dependent inverse Hall–Petch exists.

The main features of these phenomenologies are reassumed as follows:

(1) One of the most striking features of the nano-structured SiC is that they do not seem to exhibit the well-known indentation size effect, ISE,<sup>10</sup> as usually reported for most materials, that consists of the increase of hardness decreasing the applied load. In Fig. 4a, the mean hardness values of the three materials are reported as a function of applied load. While the mean hardness value at high load, 400 mN, was almost the same for the three materials, a very different behaviour was observed when the applied load was decreased. Since the reasons for ISE are still unclear,<sup>11</sup> it is difficult to explain why nano-structured ceramics do not show this phenomenon, but the implications should be kept in mind when considering contact or wear problems. The different behaviour of hardness as a function of load indicates

that the deformation mechanisms in nano-ceramics can be different from those of micro-size ceramics. In polycrystalline micro-size ceramics bulk plastic deformation is mainly due to the nucleation and spread of bulk dislocations. In the nano-sized materials the absence of ISE could indicate different deformation mechanisms, such as, for example, grain boundary sliding.

(2) This different plastic deformation mechanism is also the explanation of another impressive phenomenon which was revealed by the nanoindentation tests on these nano-ceramics: i.e. the Inverse Hall–Petch relationship. While in micro-structured ceramics hardness increase with the decrease of the grain size, in nano-structured ceramics, like previously observed also in metals, hardness decreases with the decrease of the grain size at low peak loads<sup>12</sup> (Fig. 4b). Due to the indentation size effect of the micro-sized sample, the inverse Hall–Petch relation resulted to be a load-dependent phenomenon. The repercussion of this behaviour on the material performance is well synthesized by the following statement:<sup>13</sup> “... when grain boundary sliding is dominant, grain refinement will weaken the material (inverse Hall–Petch) but when crystallographic deformation is dominant (conventional Hall–Petch), grain refinement will strengthen the material.”

The trend of the Young's modulus value, in function of the applied load, (Fig. 5), strongly resembles that of hardness. Although these phenomena need further investigations, at very low loads, the contribution of the grain boundary phase can be detected in nano-structured ceramics.

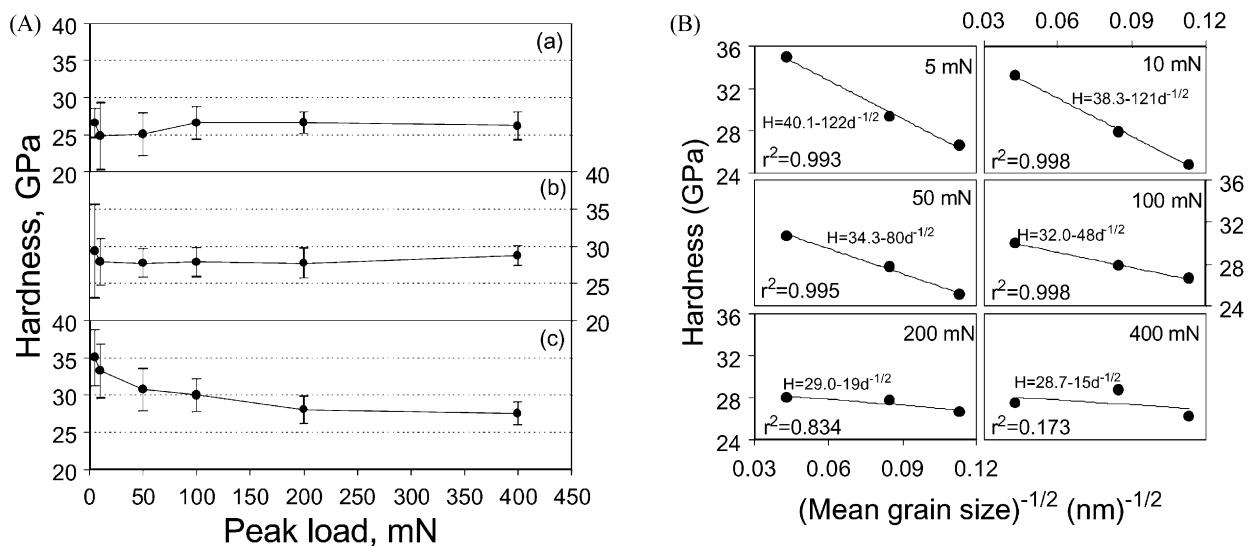


Fig. 4. A. Hardness in function of the peak load measured through nano-penetration tests on the following materials: (a) from PS powder, (b) from LS powder, (c) from commercial powder. B. Relationships between hardness and grain size at different peak loads ( $r^2$  goodness of fit).

Table 3

Compositions, characteristics of the powders and mean grain size of the alumina matrix in the hot pressed materials

Sample	Compositions vol. %	Powder mean grain size (nm) Al <sub>2</sub> O <sub>3</sub> SiC	Hot pressing T °C	M. g. s. of the alumina matrix $\mu\text{m}$
A5*	Al <sub>2</sub> O <sub>3</sub> + 5SiC	140 45	1700	0.34
A*	Al <sub>2</sub> O <sub>3</sub>	140	1450	1.2
A5	Al <sub>2</sub> O <sub>3</sub> + 5SiC	60 30	1700	0.3–0.4
A2	Al <sub>2</sub> O <sub>3</sub> + 2SiC	60 30	1670	0.4–0.5
A0.5	Al <sub>2</sub> O <sub>3</sub> + 0.5SiC	60 30	1650	~0.6
A	Al <sub>2</sub> O <sub>3</sub>	60	1450	~0.9

### 3. Selected properties of alumina–silicon carbide nano-composites

#### 3.1. Microstructure and mechanical properties

Al<sub>2</sub>O<sub>3</sub>–SiC nano-composites (Table 3) containing different amounts (0.5, 2, 5%) of ultrafine SiC and starting from different powders (SiC with 45 and 30 nm particle size) were produced and compared to monolithic alumina.<sup>8</sup> The hot pressing temperature necessary to obtain fully dense materials increased from 1450 to 1700 °C (Table 3) with increasing the amount of SiC. The mean grain size of the alumina matrix also varied greatly in an inverse relationship with the amount of SiC.

SEM micrographs in Fig. 6 show the comparison of the microstructure in alumina–silicon carbide nano-composites depending on the amount of silicon carbide.

TEM picture in Fig. 7a, evidences the morphology of alumina grains and the distribution of SiC particles. In particular SiC nanocrystals locate and agglomerate at the triple points and are embedded in grain boundary glassy phase, with composition in the Al–Si–O system (Fig. 7b). This latter phase (aluminium silicate) forms

during sintering by reaction between silica impurities present in the starting powders and some alumina and concentrates at triple points and large pockets. In some cases Al<sub>2</sub>O<sub>3</sub>–SiC boundaries are free from amorphous phase and assess strong adhesion between SiC particle and Al<sub>2</sub>O<sub>3</sub> grain.

Table 4 shows the variation of the mechanical properties. The best values of strength concern the sample that contains SiC of 45 nm, while the addition of finer particles increases the processing flaws (particle agglomeration, large alumina grains) and microcracking induced by the presence of SiC agglomerates at the grain boundaries, (Fig. 8), which overcome positive effects on strength due to the very fine microstructures of the nanocomposites.

The toughness data do not sustain any toughening mechanisms previously suggested for sub-micron sized composites, where SiC particles ranged from 100 to 300 nm and with alumina grains of 1–2  $\mu\text{m}$ .<sup>4,7</sup> Toughening is not achievable by the nanocomposite approach, when the second phase is in the tested size range.<sup>8,16</sup> Dispersoids larger than the nanometer scale are needed to improve toughness.

#### 3.2. Wear resistance

The most interesting aspect of nano-structured alumina/silicon carbide nanocomposite is related to the wear resistance and depends on the particle size of the SiC phase.<sup>17</sup> For this purpose, dry sliding wear tests using the disk-on-pin technique were carried out on two nanocomposites containing different SiC particle size:

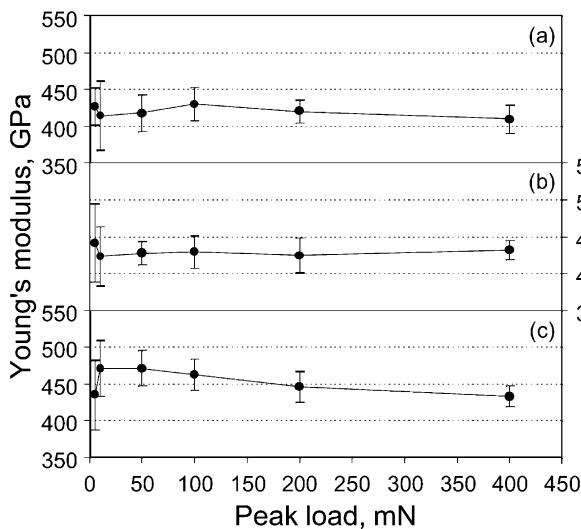


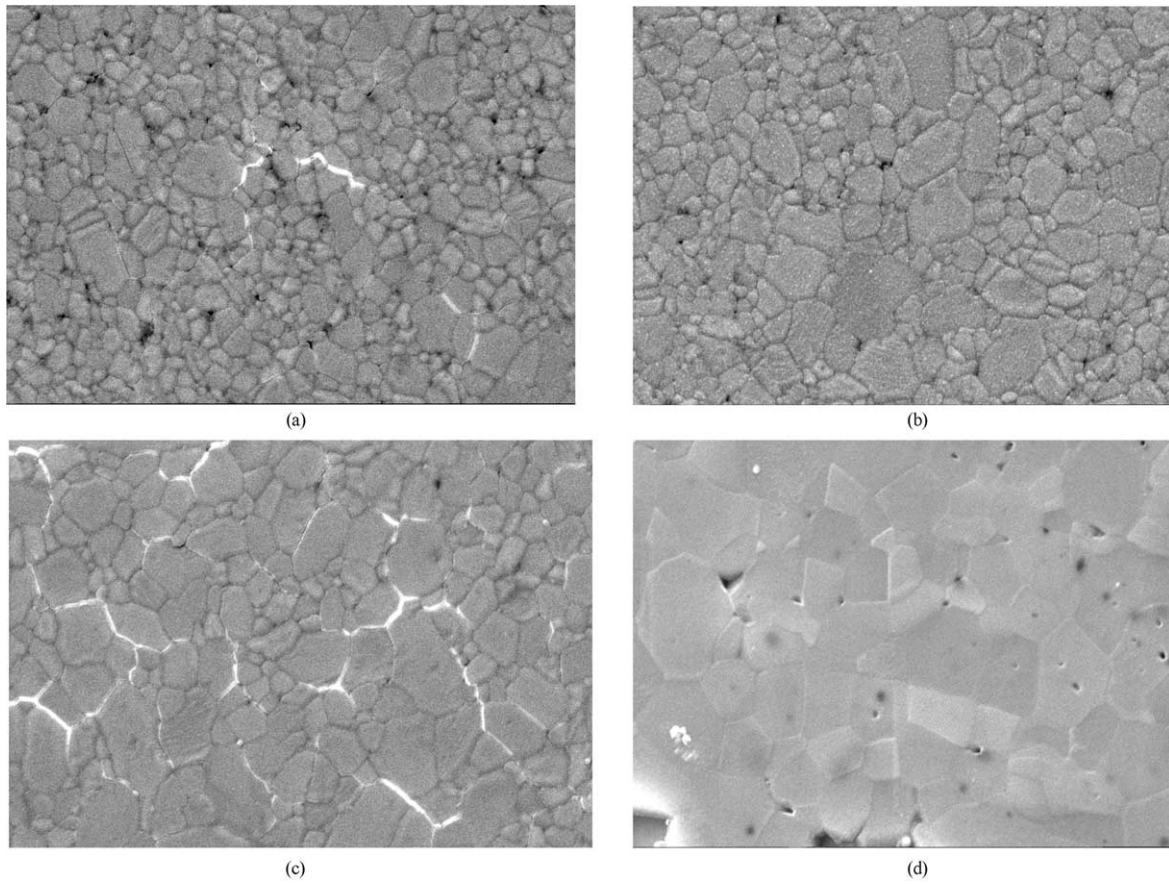
Fig. 5. Young's modulus in function of the peak load, measured through nano-penetration tests on the following materials: (a) from PS powder, (b) from LS powder, (c) from commercial powder.

Table 4

Mechanical properties of the Al<sub>2</sub>O<sub>3</sub>–SiC nanocomposites, in comparison to the values of monolithic alumina

Sample	Hardness GPa	Young's modulus GPa	Fracture Toughness MPa·m <sup>1/2</sup>	Strength MPa
A5*	20.4±0.4	357±4	3.8±0.2	642±102
A*	18.7±0.6	396±5	3.0±0.2	430±37
A5	20.1±0.4	368±4	2.9±0.1	403±29
A2	20.9±0.5	367±4	2.7±0.1	477±21
A0.5	19.1±0.4	379±4	2.9±0.2	432±75
A	18.3±0.5	380±4	3.5±0.2	575±142





Figs. 6. SEM micrograph of the hot pressed alumina-SiC nanocomposite containing the following volume% of SiC nanoparticles: (a) 5, (b) 2, (c) 0.5, (d) 0.

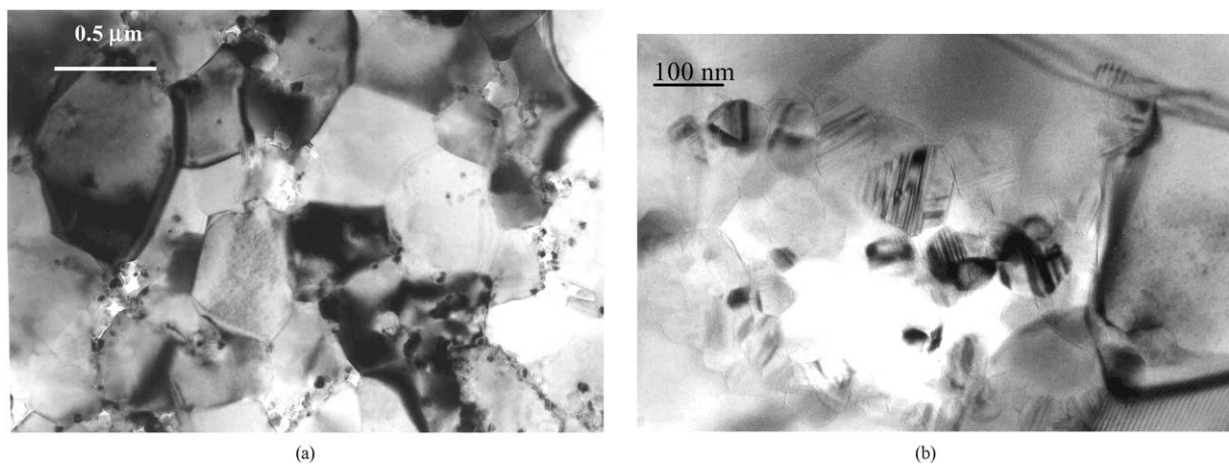


Fig. 7. (a). TEM micrograph showing the grain morphology and the distribution of SiC nanoparticles. (b) TEM micrograph evidencing the aggregation of SiC particles at triple points.

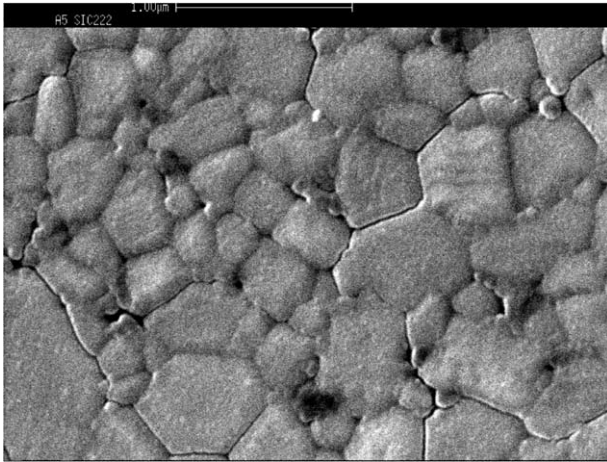


Fig. 8. Microcracking at the grain boundaries in  $\text{Al}_2\text{O}_3$ -SiC nano-composite.

$\text{Al}_2\text{O}_3 + 5 \text{ vol.}\% \text{ n-SiC (52 nm)}$   
 $\text{Al}_2\text{O}_3 + 5 \text{ vol.}\% \mu\text{-SiC (220 nm)}$

and compared to a monolithic alumina.

“Mild regime” (applied load: 20 N sliding speed: 0.05 m/s) and “severe regime” (applied load: 40 N sliding speed: 0.5 m/s) experimental conditions were adopted,<sup>17</sup> Table 5. The total sliding distance of the tests was 10 km and the radius of revolution 17 mm.

Table 5

Wear coefficient ( $10^{-6} \text{ g/km}\cdot\text{N}$ ) of the tested materials in conditions of mild regime (load 20 N, sliding speed 0.05 m/s) and of severe regime (load 40 N, sliding speed 0.5 m/s)

	Pin		Disk	
	Mild regime	Severe regime	Mild regime	Severe regime
$\text{Al}_2\text{O}_3$	0.17	73.86	1.00	1051.1
$\text{Al}_2\text{O}_3 + 5 \text{ vol.}\% \text{ n-SiC (52 nm)}$	0.13	0.61	1.5	0.50
$\text{Al}_2\text{O}_3 + 5 \text{ vol.}\% \mu\text{-SiC (220 nm)}$	0.10	2.15	2.0	1.25

The friction coefficients measured on the three materials were not different under mild regime, while under severe regime the friction coefficients of the composites were about 40% lower than that of pure alumina.

Under mild conditions, the wear rate was rather similar in the two composites and in monolithic alumina. On the contrary, under severe conditions, Table 5, the wear rates for both the composites were 3–4 orders of magnitude lower than for monolithic alumina. The results reveal also the influence of the SiC particle size: the wear coefficient is slightly lower in the composites with the finest SiC particles.

On the basis of these data and of the microstructures of the worn areas, Fig. 9 the higher wear resistance of the composites is due either to more resistant  $\text{Al}_2\text{O}_3$ /SiC interfaces, that inhibits grain boundary fracture and pullout or to the formation of a protective debris scale. In fact in the monolithic alumina, inter-, intra-granular fracture, grain pullout, grain comminution were observed, while in the two composites a compact debris layer could be beneficial for the wear resistance of the composites.<sup>18</sup> Actually, this higher resistance could be attributed to the following two factors. Firstly, as the wear in ceramic materials is usually triggered by grain boundary fracture,<sup>19</sup> the more resistant SiC–alumina interface with respect to the alumina–alumina interface<sup>20</sup> could inhibit the triggering mechanism of grain boundary fracture and pullout. Secondly, the different nature of the compact debris layer (and probably of a

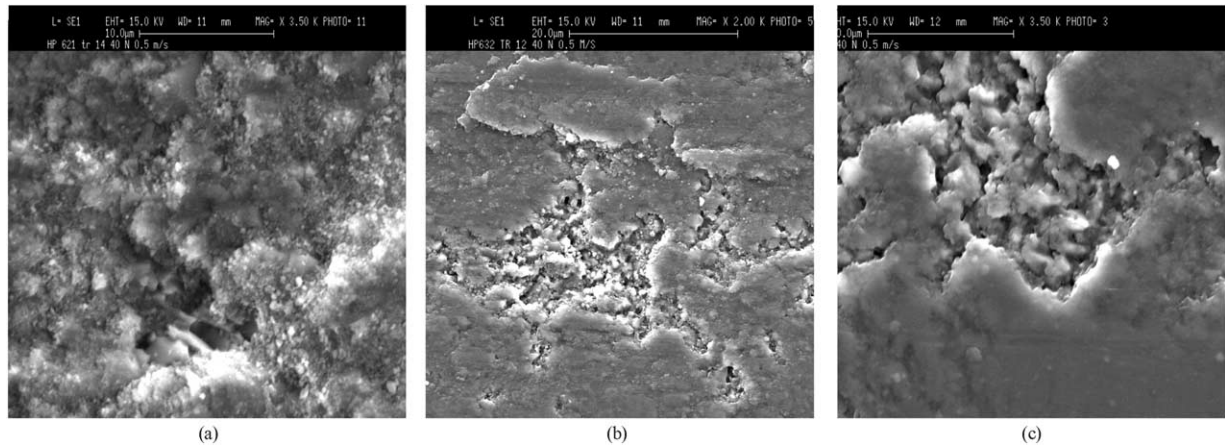


Fig. 9. SEM micrograph of the worn area after the tests under severe conditions, relative to: (a) monolithic alumina, (b)  $\text{Al}_2\text{O}_3$ -5 vol.%  $\mu\text{-SiC}$  composite (c)  $\text{Al}_2\text{O}_3$ -5 vol.% n-SiC composite.

surface silicate due to the oxidation of SiC to SiO<sub>2</sub>), which is formed during the wear of the composites, could act as a protection with regard to the underlying surface.

#### 4. Conclusions

Two laboratory-produced nano-sized SiC powders and a commercial SiC powder were characterized and processed to obtain nearly fully dense SiC materials by hot-pressing through liquid-phase sintering. The final microstructures of the nano-structured SiC materials were both very fine with a mean grain size dimension, in the best case, of about 78 nm. Besides the mean grain size, the two nano-structured SiC materials also differed in the total amount and composition of the intergranular phase. Most of the mechanical properties of the two nano-structured SiC materials were comparable to those of the material produced with a commercial SiC powder.

Nanoindentation tests were proved to be a useful tool for the characterization of these materials down to microstructural level. The salient results can be summarized as follows. Nano-structured SiC materials do not exhibit the indentation size effect in the investigated peak loads range. At very low peak loads, the contribution of the grain boundary phase can be appreciated in nano-structured materials.

This result can have profound influence in applications where just a very thin surface layer is mechanically stressed, as with contact or wear problems.

Dense Al<sub>2</sub>O<sub>3</sub>–SiC nanocomposites evidence that grain size and phase compositions depend on the starting powders and on powder processing, which are the key factors. Processing flaws limit strength. No relevant gains were observed in several mechanical properties of nanocomposites in comparison to monolithic alumina. Instead, Al<sub>2</sub>O<sub>3</sub>–SiC nanocomposites have lower friction coefficient and higher wear resistance than the pure alumina and these properties seem to be also influenced by SiC particle size.

The advantages of nano-composites are attributed either to the higher grain boundary strength. Besides, the debris layer which formed during the wear test in the nano-composites seems to be more protective. The main wear mechanisms identified were microcracking, grain fracture and grain comminution.

#### Acknowledgements

This work was carried out in the frame of the EU project BETCT97-0592-Thematic Network Nanomat. The authors thank Dr. N. Herlain (CEA-Saclay, France) and Dr. J. Grabis (Riga Technical University, Institute of Inorganic Chemistry, Latvia) for the pre-

paration of SiC nanopowders and Dr. J. Vicens (LER-MAT-ISMRA, Caen, France) for the TEM analyses.

#### References

1. Vaßen, R. and Stöver, D., Processing and properties of nano-phase non-oxide ceramics. *Mat. Sci. Eng.*, 2001, **A301**, 59–68.
2. Dong Zhan, G. and Mitomo, M., Microstructural control for strengthening of silicon carbide ceramics. *J. Am. Ceram. Soc.*, 1999, **82**(10), 2924–2926.
3. Sciti, D., Vicens, J., Herlain, N., Grabis, J. and Bellosi, A. SiC Nano-materials produced through Liquid Phase Sintering. *J. Ceram. Proc. Res.* (submitted for publication).
4. Nakahira, A. and Niihara, K., Sintering Behaviour and consolidation Process for Al<sub>2</sub>O<sub>3</sub>/SiC Nanocomposites. *J. Ceram. Soc. Jpn.*, 1992, **100**, 448–453.
5. Stearns, L. C., Zhao, J. and Harmer, M. P., Processing microstructure development in Al<sub>2</sub>O<sub>3</sub>–SiC nanocomposites. *J. Europ. Ceram. Soc.*, 1992, **10**, 473.
6. Zhao, J., Stearns, L. C., Harmer, M. P., Chan, H. M. and Miller, G. A., Mechanical behaviour of alumina-silicon carbide nanocomposites. *J. Am. Ceram. Soc.*, 1993, **76**, 503–510.
7. Carroll, L., Sternitzke, M. and Derby, R., Silicon carbide particle size effects in alumina-based nanocomposites. *Acta Mater.*, 1996, **44**(11), 4543–4552.
8. Sciti, D., Vicens, J. and Bellosi, A., Microstructure and properties of alumina–SiC nanocomposites prepared from ultrafine powders. *J. Mat. Sci.*, 2002, **37**, 3747–3758.
9. Sciti, D., Guicciardi, S. and Bellosi, A., Effect of annealing treatments on microstructure and toughness of liquid phase sintered silicon carbide. *J. Eur. Ceram. Soc.*, 2001, **21**, 621–632.
10. McColm, I. J., *Ceramic Hardness*. Plenum Press, New York, USA, 1990.
11. Swadener, J. G., George, E. P. and Pharr, G. M., The correlation of the indentation size effect measured with indenters of various shapes. *J. Mech. Phys. of Solids*, 2002, **50**, 681–694.
12. Guicciardi, S., Sciti, D., Melandri, C., and Bellosi, A. Nano-indentation characterization of nano-sized liquid phase sintered SiC ceramics. *J. Am. Ceram. Soc.* (submitted for publication).
13. Hahan, H., Mondal, P. and Padmanabhan, K. A., Plastic deformation of nanocrystalline materials. *Nanostructured Materials*, 1997, **9**, 603–606.
14. Drugan, W. J. and Willis, J. R., A micromechanics-based non-local constitutive equation and estimates of representative volume element size for elastic composites. *J. Mech. Phys. Solids*, 1996, **44**, 497–524.
15. Krajcinovic, D. Damage mechanics, North-Holland series in Applied mathematics and mechanics, vol. 41, Elsevier Science Publishers, Amsterdam, The Netherlands, 1996, p. 231.
16. Pezzotti, G. and Muller, W. H., Strengthening mechanisms in Al<sub>2</sub>O<sub>3</sub>/SiC nanocomposites. *Comp. Mater. Sci.*, 2001, **22**, 155–168.
17. Guicciardi, S., Sciti, D., Melandri, C. and Bellosi, A., Dry sliding wear of Al<sub>2</sub>O<sub>3</sub>–SiC submicro- and nano-composites. *J. Am. Ceram. Soc.* (Submitted for publication).
18. Randall, N. X. and Harris, A., Nanoindentation as a tool for characterising the mechanical properties of tribological transfer films. *Wear*, 2000, **245**, 196–203.
19. Fischer, T. E., Zhu, Z., Kim, H. and Shin, D. S., Genesis and role of wear debris in sliding wear of ceramics. *Wear*, 2000, **245**, 53–60.
20. Jiao, S., Jenkins, M. L. and Davidge, R. W., Interfacial fracture energy-mechanical behaviour relationship in Al<sub>2</sub>O<sub>3</sub>/SiC and Al<sub>2</sub>O<sub>3</sub>/TiN nanocomposites. *Acta Mater.*, 1997, **45**, 149–156.